SCIENCE CHINA
Information Sciences

• LETTER •

January 2026, Vol. 69, Iss. 1, 119302:1–119302:2
https://doi.org/10.1007/s11432-025-4620-6

Multi-frequency ultra-wideband channel measurements and characterization for 6G IIoT communication systems

Ziheng LI[1†], Shudong ZHOU[1†], Yu LIU[1,2*], Xinrong ZHANG[1], Jie HUANG[2,3], Ji BIAN[4] & Rui WANG[5]

[1]*School of Integrated Circuits, Shandong University, Jinan 250101, China*
[2]*National Mobile Communications Research Laboratory, School of Information Science and Engineering, Southeast University, Nanjing 211189, China*
[3]*Purple Mountain Laboratories, Nanjing 211111, China*
[4]*School of Information Science and Engineering, Shandong Normal University, Jinan 250358, China*
[5]*Shandong Taikai Disconnector Co., Ltd., Taian 271000, China*

Received 4 April 2025/Revised 22 August 2025/Accepted 29 September 2025/Published online 4 January 2026

Citation Li Z H, Zhou S D, Liu Y, et al. Multi-frequency ultra-wideband channel measurements and characterization for 6G IIoT communication systems. Sci China Inf Sci, 2026, 69(1): 119302, https://doi.org/10.1007/s11432-025-4620-6

The close integration of the sixth-generation (6G) communications and the Internet of Things (IoT) technologies has driven the widespread application of the industrial IoT (IIoT). As a communication technology-driven manufacturing paradigm, the IIoT can effectively overcome the limitations of traditional wired connections in terms of deployment cost and maintenance efficiency [1–3]. However, industrial environments pose distinct challenges to the IIoT communication field, particularly due to complex multipath propagation, rich scattering environments, and significant path loss (PL). These factors can often lead to unpredictable signal behavior, making the design and implementation of reliable communication networks complex. Therefore, understanding these unique characteristics and modeling the IIoT channels are critical for deploying and optimizing the IIoT communication systems.

IIoT channel modeling based on measurement data can align with actual scenarios and exhibit higher robustness. Most existing channel measurements in IIoT scenarios were carried out in relatively simple environments, such as general factories, laboratories, and offices, with little focus on real-world measurements in more complex industrial settings. Additionally, the measurement frequency bands were relatively limited. Furthermore, there was a lack of comparison across multiple frequencies and bandwidths, as well as insufficient consideration of how equipment density affects the channel in an IIoT environment.

To address these challenges, this study conducts multi-frequency ultra-wideband channel measurements in a smart factory. Our main contributions are as follows. (1) Ultra-wideband (UWB) IIoT channel measurements and characteristic analysis under typical scenarios are conducted across multiple frequencies, and the impacts of different device densities on key channel characteristics are elaborated. (2) Multipath clustering and tracking are performed on IIoT channels using power delay profiles (PDPs). The mechanism by which dynamic metallic equipment affects abrupt changes in cluster counts is clarified based on the Saleh-Valenzuela (S-V) model. (3) A new dual-slope PL model incorporating equipment density is proposed, which accurately characterizes the nonlinear relationship between PL, metal density, distance, and frequency.

IIoT channel measurement. The IIoT channel measurements were performed in a smart factory of Tai Kai Group in Shandong Province, China. The factory is approximately 220 m long and 160 m wide and has a complex internal environment that includes numerous metallic scatterers, moving equipment, and operating machinery. The vector signal transceiver (VST) was used for channel measurements. The measurement equipment is illustrated in Figure 1. The transceiver process of the VST is presented in Appendix A.1. To meet different testing requirements, during the measurement period, the factory was divided into dense equipment areas and sparse equipment areas as shown in Figure 1. See Appendix A.2 for the specific measurement process.

Measurement data processing. During the measurement data processing, the channel impulse response (CIR) is firstly obtained by calibrating out effects of the system response from the raw measurement data. See Appendix B.1 for the processing process of CIR. The PDP obtained through CIR preprocessing can clearly demonstrate the relationship between the received signal power and the arrival time delay, which can be given by

$$P_{\mathrm{PDP}}(\tau) = \mathbb{E}\left[|h(\tau)|^2\right], \tag{1}$$

where τ is the time delay, $h(\tau)$ is the CIR at a time delay of τ, and $\mathbb{E}[\cdot]$ is the expectation operator used for averaging over different CIRs. The peak search algorithm is used to extract multipath components (MPCs) from the PDP with a threshold determined by the maximum power and noise floor. Based on this, the typical channel characteristics are calculated. More details about the characteristic calculation formulas can be found in Appendix B.2.

Model description. In IIoT communication, two commonly used PL models are the alpha-beta-gamma (ABG) PL model [4] and the

* Corresponding author (email: yuliu@sdu.edu.cn)
† These authors contributed equally to this work.

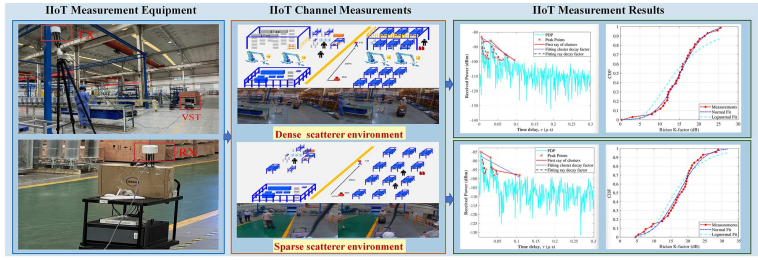

Figure 1 (Color online) IIoT channel measurement and measurement results.

close-in (CI) free space PL model [5]. Under single-frequency conditions, the ABG model simplifies to the floating-intercept (FI) model. In this study, a new PL model incorporating equipment density was introduced based on the earlier work, and it is defined as follows:

$$\mathrm{PL} = \begin{cases} (10+\rho)n_1 \log_{10}(d) + A_1\rho + 20\log_{10}(f_c), & d \leqslant r_{bp}, \\ (10+\rho)n_2 \log_{10}(d) + A_2\rho + 20\log_{10}(f_c), & d > r_{bp}, \end{cases} \quad (2)$$

where d represents the distance between the Tx and Rx. r_{bp} is the threshold distance used to distinguish between the near- and far-field regions, which was set to 10 m in this study; and ρ is the number of pieces of equipment per square meter, and to obtain the value of ρ, communication with the factory staff is required for confirmation. Parameters A_1, A_2, n_1, and n_2 are the fitting parameters for PL, and they are obtained through fitting measurement data.

The root mean square delay spread (RMS DS) and Rician K-factor (K-factor) are often fitted by normal distribution, lognormal distribution, and exponential distribution. The Akaike information criterion (AIC) method and the Bayesian information criterion (BIC) method were used to identify the best-fitting model. The specific formulas can be found in Appendix C.

Measurement results and analysis. The PDP was analyzed through clustering using the bubble clustering algorithm, and the parameters of the S-V channel model were optimized and fitted based on the minimum mean square error (MMSE) criterion. The clustering results are presented in Figure 1, where it can be seen that the decay rates of the clusters followed an exponential distribution. More details about statistical results can be found in Appendix D.1.

The coefficient of determination R2 was used as an evaluation metric to validate the model fitting quality. According to the R2 values (see Tables D1 and D2 in Appendix D.2), the dual-slope model achieved the best fit for PL in complex factory environments. The details of the comparison results are provided in Appendix D.2.

The fitting results of RMS DS are presented in Tables D4 and D5 in Appendix D.3, where it can be seen that there were significant differences in the optimal models across different equipment density scenarios. Based on the AIC and BIC values, the normal distribution was identified as the best-fitting model for the dense equipment environments. In contrast, the lognormal distribution was considered the best-fitting model for the sparse equipment environments.

The fitting results of the K-factor CDF in the dense and sparse equipment scenarios obtained in this study are illustrated in Figure 1, where it can be seen that both of them followed a normal distribution. In addition, the measurement results indicate that equipment density also has a significant impact on channel correlation. More details about statistical results can be found in Appendix D.5.

Conclusion. This study has conducted UWB IIoT channel measurements in two typical scenarios and has elaborated for the first time the impacts of different device densities on channel characteristics. The accurate clustering and tracking of multipaths in IIoT channels have been achieved using PDPs. By fitting the parameters of the S-V model, a negative correlation between device density and ray decay rate was identified. Furthermore, a dual-slope PL model incorporating device density has been innovatively proposed, and compared with other models, its fitting accuracy has been greatly improved. This study provides key technical support for the link design, coverage planning, and performance optimization of IIoT communication systems.

Acknowledgements This work was supported by National Natural Science Foundation of China (Grant Nos. 62471279, 62271147, 62101311), Natural Science Foundation of Shandong Province (Grant No. ZR2024MF062), Future Plan Program for Young Scholars of Shandong University, the Open Research Fund of National Mobile Communications Research Laboratory, Southeast University (Grant No. 2025D03), and Innovation and Technology Support Program for Young Scholars of Colleges and Universities in Shandong Province (Grant No. 2022KJ009).

Supporting information Appendixes A–D. The channel data can be available at https://github.com/371502200001236834/IIOT-channel-measurement-data. The supporting information is available online at info.scichina.com and link.springer.com. The supporting materials are published as submitted, without typesetting or editing. The responsibility for scientific accuracy and content remains entirely with the authors.

References

1 You X H, Wang C X, Huang J, et al. Towards 6G wireless communication networks: vision, enabling technologies, and new paradigm shifts. Sci China Inf Sci, 2021, 64: 110301
2 Nguyen D C, Ding M, Pathirana P N, et al. 6G Internet of Things: a comprehensive survey. IEEE Int Things J, 2021, 9: 359–383
3 Wang C X, Lv Z, Gao X, et al. Pervasive wireless channel modeling theory and applications to 6G GBSMs for all frequency bands and all scenarios. IEEE Trans Veh Technol, 2022, 71: 9159–9173
4 Doone M G, Cotton S L, Matolak D W, et al. Pedestrian-to-vehicle communications in an urban environment: channel measurements and modeling. IEEE Trans Antennas Propagat, 2019, 67: 1790–1803
5 Zhang J H, Wang Y J, Tang P, et al. Overview of research on channel characteristics and modeling in the IIoT scenarios. Chinese J Radio Sci, 2023, 38: 3–14